Exact solution for the bending deformations of layered magneto-electro-elastic laminates based on thin-plate formulation

Mei-Feng Liu

***Abstract*—In this paper, a rather compact differential equation governing the bending behavior of a magneto-electro-elastic (MEE) rectangular thin plate is introduced, in particular, the exact solutions for the deformation response of laminated BaTiO3-CoFe2O4 composites subjected to certain types of surface loads are analytically obtained. Due to the omission of the transverse shear deformation and rotatory inertia assumed in Kirchhoff thin-plate theory, the governing equation can accordingly be expressed in terms of the transverse displacement only. As a result, the structural characteristics such as elastic displacements, electric potential and magnetic induction for a magneto-electro-elastic (MEE) rectangular plate can be carried out in a theoretical approach. For a laminate MEE composite, the material constants can be uniquely determined by the volume-fraction (v.f.) of the piezoelectric constituent BaTiO3, and are tabulated with 25% offset of the volume-fraction. According to the specified boundary conditions imposed on the MEE thin plate, the deformation variations with closed-circuit electric restriction are evaluated analytically in the present study. The results obtained in this paper by using the proposed model can be shown to have good agreements with the other available research works, however, with the advantage that the present study indeed provides a much simpler way in seeking the analytic solutions for the interactively coupled quantities of a layered MEE medium.**

***Index Terms*—Layered structures, Mechanical properties, Analytical modelling**

I. INTRODUCTION

It is well-known that structure made of piezoelectric materials can produce voltage when external stress is applied, nevertheless, it will also induce stress when voltage difference is implemented across the structure. Parallel to the piezoelectricity, piezomagnetizm can intrinsically be characterized by interactive couplings between system's magnetic polarization and mechanical strain, i.e., in a piezomagnetic medium, one may induce a spontaneous magnetic moment by applying physical stress, or reversely obtain a physical deformation by applying a magnetic field. Composites structures consist of layered piezoelectric and piezomagnetic components, which can be referred as one kind of the magneto-electro-elastic (MEE) material, possesses the ability to convert energy of magnetism, electricity or elasticity into another form. The MEE material also exhibits a specific magneto-electric effect which is not appeared in a single-phase piezoelectric or piezomagnetic material. Surprisingly, in some cases the magneto-electric effect of MEE composites can even be obtained two orders larger than that of a single-phase magneto-electric material with highest magneto-electro coefficient [1]. Due to these multiphase properties, the MEE material have been found increasing applications in making efficient smart and intelligent structures such as magnetic field probes, electric packing, acoustic, hydrophones, medical ultrasonic imaging and so on.

For the past few years, systematic investigations either in determining the material coefficient of such new type material or in analyzing the static or dynamic behavior under certain external conditions are vigorously proposed by many professional engineers and scientists. Li [2] studied the average magneto-electro-elastic fields in the multi-inclusion embedded in an infinite matrix, and estimated the effective magneto-electro-elastic moduli of piezoelectric-piezomagnetic composites for both BaTiO3 fiber reinforced CoFe2O4 and BaTiO3-CoFe2O4 laminate. It has been shown that the magneto-electro coupling demonstrated by magneto-electro coefficients vary with the volume faction of BaTiO3 and have opposite signs for fibrous and laminated composites, respectively. Pan [3] obtained the exact solution for three dimensional, anisotropic, linear magneto-electro-elastic, simply-supported and multilayered rectangular plates under static loadings. It is stated that even for relatively thin plate, responses from an internal load are quite different to those from a surface load. Chen et. al. [4] establish a micro-mechanical model to evaluate the effective properties of layered magneto-electro-elastic composites and the linear coupling effect between elasticity, electricity and magnetism of the MEE composite is accordingly derived. In their study, numerical results for a BaTiO3-CoFe2O4 composite with 2-2connectivi are obtained, and the dependences of magneto-electro-elastic coefficients, the so-called product properties, of the composite on the volume fraction of BaTiO3 are clearly depicted. Wang and Shen [5] extended their previous works on piezoelectric media to study the general solution of three-dimensional problems in transversely isotropic magneto-electro-elastic media through five newly introduced potential functions. Chen and Lee [6] simplified the governing equations of the linear theory for the magneto-electro-thermal-elastic plate with transverse isotropy by introducing two displacement functions and stress functions. In their study, two new state space equations are established while selecting certain physical quantities as the basic unknowns. Wang et. al. [7] performed a state vector formulation for the three dimensional, orthotropic and linearly magneto-electro-elastic multiple layered plate and expressed the basic unknowns by collecting not only the displacement, electric potential and magnetic potential but also some of the stresses, electric displacements, and magnetic induction. A boundary integral formulation for the plane problem of magneto-electro-elastic media are

Mei-Feng Liu, Dept. of Financial and Computational Mathematics, I-Shou University, Kaohsiung, Taiwan R.O.C, +886-6577711ext.5625,

performed by Ding and Jiang [8] using strict differential operator theory. They obtained the fundamental solutions for an infinite MEE plane in terms of four harmonic functions which satisfied a set of reduced second order partial differential equation for distinct eigenvalues case. Guan and He [9] derived the fundamental equation for the plane problem of a transversely isotropic magneto-electro-elastic media by applying the Almansi's theorem and expressed all physical quantities by four harmonic functions for distinct and non-distinct cases.

In this study, a rather simple analytic solution for the deformations of the magneto-electro-elastic (MEE) rectangular plate under certain type of applied loads acting on the top surfaces are derived. By imposing the Kirchhoff thin-plate hypothesis on the plate constituent, the governing equation in terms of only the transverse displacement of the plate can be obtained and therefore a rather compact form indicating the multiple effects between elasticity, electricity and magnetism of the plate can be successfully presented. The MEE plate is chose to be made of the two-layered BaTiO3-CoFe2O4 laminate, which can be thought as a transversely isotropic magneto-electro-elastic medium and the material coefficients for such continuum can be expressed uniquely by introducing the volume-fraction of BaTiO3 in the layered composite. The corresponding deformation analysis regarding the elastic displacements, electric potential and magnetic induction of the MEE thin plate is evaluated through the formulation mentioned in this study. Some comparisons with previous literatures are made and great agreements are reached which directly validate the proposed simplification for the MEE modeling.

II. Formulations

For a Magneto-Electro-Elastic (MEE) thin plate made of two-layered $BaTiO_3$-$CoFe_2O_4$ laminate, the fundamental Kirchhoff hypothesis for the small-deflection of simple bending problem can be applied, and thus the transverse shear deformations and rotary inertias can be neglected, also the transverse shear strains are negligible. In accordance with the assumptions that in-plane electric fields and magnetic fields in a very thin medium can be ignored [10], that is, only the transverse electric, E_3, and magnetic field, H_3, are under consideration, the following governing equation for the bending problem can be found [11]

$$\left\{D\nabla^4 w + E\nabla^4 w + M\nabla^4 w\right\} = P(x,y)\,, \tag{1}$$

where $D \equiv \dfrac{c_{11}h^3}{12}$ represents the plate rigidity, $E \equiv \dfrac{e_{31}h^3}{12}\cdot\dfrac{\Delta_1}{\Delta}$ denotes the effective rigidities induced by electricity, $M \equiv \dfrac{q_{31}h^3}{12}\cdot\dfrac{\Delta_2}{\Delta}$ is the corresponding effective rigidities cause by magnetism and $P(x,y)$ denotes the applied load acting on the top surface. Herein h is the plate thickness, $\Delta \equiv \varepsilon_{33}\mu_{33} - d_{33}^2$, $\Delta_1 \equiv (e_{31}\mu_{31} - d_{33}q_{33})$ and $\Delta_2 \equiv -(\varepsilon_{33}q_{31} - d_{33}e_{31})$ are extra-defined parameters aiming to simplify the derivations; c_{ij}, e_{ij}, q_{ij}, d_{ij} and μ_{ij} are the elastic, dielectric, piezoelectric, piezomagnetic, magnetoelectric, and magnetic constants, respectively. It should be noted the relation $c_{11} = c_{12} + 2c_{66}$ for transversely isotropic material is adopted in the above equation. As it can be also learned from Ref. [11], the reduced extended traction vectors can be stated as follows,

$$\sigma_x = c_{11}\left(-z\frac{\partial^2 w}{\partial x^2}\right) + c_{12}\left(-z\frac{\partial^2 w}{\partial y^2}\right) + e_{31}\frac{\partial \phi}{\partial z} + q_{31}\frac{\partial \psi}{\partial z}$$

$$\sigma_y = c_{12}\left(-z\frac{\partial^2 w}{\partial x^2}\right) + c_{11}\left(-z\frac{\partial^2 w}{\partial y^2}\right) + e_{31}\frac{\partial \phi}{\partial z} + q_{31}\frac{\partial \psi}{\partial z}\,, \tag{2}$$

$$\tau_{xy} = c_{66}\left(-z\frac{\partial^2 w}{\partial x \partial y} - z\frac{\partial^2 w}{\partial y \partial x}\right) = -2c_{66}z\frac{\partial^2 w}{\partial x \partial y}$$

$$D_z = e_{31}\frac{\partial u}{\partial x} + e_{31}\frac{\partial v}{\partial y} - \varepsilon_{33}\frac{\partial \phi}{\partial z} - d_{33}\frac{\partial \psi}{\partial z}\,, \tag{3}$$

$$B_z = q_{31}\frac{\partial u}{\partial x} + q_{31}\frac{\partial v}{\partial y} - \varepsilon_{33}\frac{\partial \phi}{\partial z} - \mu_{33}\frac{\partial \psi}{\partial z}\,. \tag{4}$$

Meanwhile, the following expression for the electric potential and magnetic potential can be derived,

$$\frac{\partial \varphi}{\partial z} = -\frac{\Delta_1}{\Delta}z\nabla^2 w + \varphi_1(x,y)\,, \tag{5}$$

$$\frac{\partial \psi}{\partial z} = -\frac{\Delta_2}{\Delta}z\nabla^2 w + \psi_1(x,y)\,, \tag{6}$$

where $\varphi_1(x,y)$ and $\psi_1(x,y)$ represent the variations of electric field and magnetic field in the thickness direction while the plate is under deformation, and are both independent of z variable.

In seeking for the solution to Eq. (1), we can assume the following expression for the transverse deflection of the MEE plate,

$$w(x,y) = \sum_{m=1}^{\infty}\sum_{n=1}^{\infty} A_{mn}X_m(x)Y_n(y)\,, \tag{7}$$

where $X_m(x)$ and $Y_n(y)$ are the homogeneous solutions of Eq. (1) and can be determined according to the assigned boundary conditions. Some mode shapes and corresponding eigenvalues with respect to commonly seen boundary conditions are tabulated in Table 1 as a reference. It should be noted that the mode shapes $X_m(x)$ and $Y_n(y)$ not only satisfy the corresponding boundary conditions but also possess the intrinsic orthogonality, i.e., we will have

$$\int_0^{L_x} X_m(x)X_M(x)dx = \begin{Bmatrix} \|X_m(x)\|, & if\ m = M \\ 0, & if\ m \neq M \end{Bmatrix} \equiv \|X_m(x)\|\delta_{mM}\,, \tag{8}$$

and

$$\int_0^{L_y} Y_n(y)Y_N(y)dy = \begin{Bmatrix} \|Y_n(y)\|, & if\ n = N \\ 0, & if\ n \neq N \end{Bmatrix} \equiv \|Y_n(y)\|\delta_{nN}\,, \tag{9}$$

where L_x and L_y denotes the plate lengths along x and y directions. After $X_m(x)$ and $Y_n(y)$ are determined, we can further expand the applied load on the top surface of the plate into the generalized double Fourier series as

$$P(x,y) = \sum_{m=1}^{\infty}\sum_{n=1}^{\infty} p_{mn}X_m(x)Y_n(y)\,, \tag{10}$$

in which the Fourier coefficient p_{mn} can be determined as follows

$$p_{mn} = \frac{1}{\|X_m(x)\|\|Y_n(y)\|}\int_0^{L_x}\int_0^{L_y} P(x,y)X_m(x)Y_n(y)dxdy\,. \quad (11)$$

By substituting Eq. (7) and Eq. (10) into Eq. (1) and collecting the constant term, we can have the following equation

$$(D+E+M)\left(\alpha_m^4 + 2\alpha_m^2\beta_n^2 + \beta_n^4\right)A_{mn} = p_{mn}\,, \quad (12)$$

where α_m and β_n are the corresponding eigenvalues associated to the specific boundary conditions. Furthermore, the magnitude of the transverse deflection, A_{mn}, can be determined, i.e.,

$$A_{mn} = \frac{p_{mn}}{(D+E+M)\left(\alpha_m^4 + 2\alpha_m^2\beta_n^2 + \beta_n^4\right)}\,. \quad (13)$$

Thus we have the exact solution for the transverse deflection due to applied load

$$w(x,y) = \sum_{m=1}^{\infty}\sum_{n=1}^{\infty}\frac{p_{mn}}{(D+E+M)\left(\alpha_m^4 + 2\alpha_m^2\beta_n^2 + \beta_n^4\right)}X_m(x)Y_n(y)\,, \quad (14)$$

and the exact solution for the mechanical displacements along x- and y- directions can be expressed as

$$u = -z\frac{\partial w}{\partial x} = \sum_{m=1}^{\infty}\sum_{n=1}^{\infty}\frac{-p_{mn}}{(D+E+M)\left(\alpha_m^4 + 2\alpha_m^2\beta_n^2 + \beta_n^4\right)}zX'_m(x)Y_n(y)\,, \quad (15)$$

$$v = -z\frac{\partial w}{\partial y} = \sum_{m=1}^{\infty}\sum_{n=1}^{\infty}\frac{-p_{mn}}{(D+E+M)\left(\alpha_m^4 + 2\alpha_m^2\beta_n^2 + \beta_n^4\right)}zX_m(x)Y'_n(y) \quad (16)$$

Table 1: Mode shapes and the corresponding eigenvalues for specified boundary conditions

Boundary Conditions	Mode shape $X_m(\xi)$	Eigevalue α_m
Pinned-Pinned	$X_m(\xi) = \sin(\frac{m\pi}{L})\xi$	$\alpha_m = \frac{m\pi}{L_x}$, $m = 1,2,3,\ldots$
Fixed-Pined	$X_m(\xi) = \cosh\alpha_m\xi - \cos\alpha_m\xi - \gamma_m(\sinh\alpha_m\xi - \sin\alpha_m\xi)$ where γ_1=1.000777, γ_2=1.000001, γ_3=1.000000	$\alpha_1 = \frac{3.926602}{L}$, $\alpha_2 = \frac{7.068583}{L}$, $\alpha_3 = \frac{10.210176}{L}$
Fixed-Free	$X_m(\xi) = \cosh\alpha_m\xi - \cos\alpha_m\xi - \gamma_m(\sinh\alpha_m\xi - \sin\alpha_m\xi)$ where γ_1=0.734096, γ_2=1.018466, γ_3=0.999225	$\alpha_1 = \frac{1.875104}{L}$, $\alpha_2 = \frac{4.694091}{L}$, $\alpha_3 = \frac{7.854757}{L}$
Fixed-Fixed	$X_m(\xi) = \cosh\alpha_m\xi - \cos\alpha_m\xi - \gamma_m(\sinh\alpha_m\xi - \sin\alpha_m\xi)$ where γ_1=0.982502, γ_2=1.000777, γ_3=0.999966	$\alpha_1 = \frac{4.730041}{L_x}$, $\alpha_2 = \frac{7.853205}{L_x}$, $\alpha_3 = \frac{10.995607}{L_x}$
Free-Free	$X_m(\xi) = \cosh\alpha_m\xi + \cos\alpha_m\xi - \gamma_m(\sinh\alpha_m\xi + \sin\alpha_m\xi)$ where γ_1=0.982502, γ_2=1.000777, γ_3=0.999966	$\alpha_1 = \frac{4.730041}{L_x}$, $\alpha_2 = \frac{7.853205}{L_x}$, $\alpha_3 = \frac{10.995607}{L_x}$

As for the electric boundary conditions and magneto boundary conditions specified on the top and bottom surfaces of the plate, there are normally two kinds of cases to be discussed.

Case I: Closed-circuit, i.e., $\phi(x,y,\pm h/2) = 0$ *and* $\psi(x,y,\pm h/2) = 0$

By carrying out the anti-derivatives for Eq. (5) and Eq. (6), we can have the following expressions for electric potential and magnetic potential as

$$\varphi(x,y,z) = -\frac{\Delta_1}{2\Delta}z^2\nabla^2 w(x,y) + z\varphi_1(x,y) + \varphi_0(x,y) \quad (17)$$

$$\psi(x,y,z) = -\frac{\Delta_2}{2\Delta}z^2\nabla^2 w(x,y) + z\psi_1(x,y) + \psi_0(x,y) \quad (18)$$

since $\phi(x,y,\pm h/2) = 0$, after solving the above two equations, one can get

$\varphi_1(x,y) = 0$ and $\varphi_0(x,y) = \frac{\Delta_1}{2\Delta}(h/2)^2\nabla^2 w(x,y)$,

thus the exact solution for the electric potential due to applied load can be expressed as

$$\varphi(x,y,z) = -\frac{\Delta_1}{2\Delta}z^2\nabla^2 w(x,y) + \frac{\Delta_1}{2\Delta}(h/2)^2\nabla^2 w(x,y)\,. \quad (19)$$

By the same token, we can have the following exact solution for the magnetic potential due to applied load as

$$\psi(x,y,z) = -\frac{\Delta_2}{2\Delta}z^2\nabla^2 w(x,y) + \frac{\Delta_2}{2\Delta}(h/2)^2\nabla^2 w(x,y)\,. \quad (20)$$

Case II: Open-circuit, i.e., $D_z(x,y,\pm h/2) = 0$ *and* $B_z(x,y,\pm h/2) = 0$

Substituting Eqs. (5)-(6) and Eqs. (15)-(16) into Eqs. (3) and (4), the solutions for the electric displacement and magnetic induction in thickness direction can be expressed as

$$D_z = \left(-e_{31} + \varepsilon_{33}\frac{\Delta_1}{\Delta} + d_{33}\frac{\Delta_2}{\Delta}\right)z\nabla^2 w - \varepsilon_{33}\varphi_1(x,y) - d_{33}\psi_1(x,y)\,, \quad (21)$$

$$B_z = \left(-q_{31} + \varepsilon_{33}\frac{\Delta_1}{\Delta} + \mu_{33}\frac{\Delta_2}{\Delta}\right)z\nabla^2 w - \varepsilon_{33}\varphi_1(x,y) - \mu_{33}\psi_1(x,y) \quad (22)$$

therefore, the open-circuit conditions will lead to

$$D_z(x,y,h/2) = \left(-e_{31} + \varepsilon_{33}\frac{\Delta_1}{\Delta} + d_{33}\frac{\Delta_2}{\Delta}\right)h/2\nabla^2 w - \varepsilon_{33}\varphi_1(x,y) - d_{33}\psi_1(x,y) = 0 \quad (23)$$

$$D_z(x,y,-h/2) = -\left(-e_{31} + \varepsilon_{33}\frac{\Delta_1}{\Delta} + d_{33}\frac{\Delta_2}{\Delta}\right)h/2\nabla^2 w - \varepsilon_{33}\varphi_1(x,y) - d_{33}\psi_1(x,y) = 0 \quad (24)$$

and

$$B_z(x,y,h/2) = \left(-q_{31} + d_{33}\frac{\Delta_1}{\Delta} + \mu_{33}\frac{\Delta_2}{\Delta}\right)(h/2)\nabla^2 w - d_{33}\varphi_1(x,y) - \mu_{33}\psi_1(x,y) = 0 \quad (25)$$

$$B_z(x,y,-h/2) = -\left(-q_{31} + d_{33}\frac{\Delta_1}{\Delta} + \mu_{33}\frac{\Delta_2}{\Delta}\right)(h/2)\nabla^2 w - d_{33}\varphi_1(x,y) - \mu_{33}\psi_1(x,y) = 0\,. \quad (26)$$

In viewing of Eq. (23) through Eq. (26), it can be found that these four equations cannot provide any information about determining the expressions for $\varphi_1(x,y)$ and $\psi_1(x,y)$, nor for the terms $\varphi_0(x,y)$ and $\psi_0(x,y)$. This is because the variations of electric displacement and magnetic displacement along thickness direction are vanished under the proposed methodology, i.e., $\frac{\partial D_z}{\partial z} = \frac{\partial B_z}{\partial z} = 0$, therefore it is expected to see the linear dependency of these two quantities on the z variable. In that sense, open-circuit boundary will result in a trivial solution with the displacement components approaching to zero and makes the expressions of $\varphi_1(x,y)$ and $\psi_1(x,y)$ being negligible as can be detected from Eqs.

(21) and (22). As a result, two more boundary conditions will be needed in order to resolve the expressions for the terms $\varphi_0(x,y)$ and $\psi_0(x,y)$. For that reason, in this study, we don't specifically focus on the open-circuit case and only adopt the closed-circuit boundary condition as our numerical examples discussed in the next section.

It should be noted that the in-plane electric fields and magnetic fields can be ignored if the plate thickness is very small (e.g. $h<10L_x$), and only the transverse electric field, E_3, and magnetic field, H_3, are related to the electric potential φ and magnetic potential ψ in the follow form according to the Maxwell's equations.

$$E_z \equiv -\frac{\partial \phi}{\partial z} = \frac{\Delta_1}{\Delta} z\nabla^2 w - \varphi_1(x,y), \tag{27}$$

$$H_z \equiv -\frac{\partial \psi}{\partial z} = \frac{\Delta_2}{\Delta} z\nabla^2 w - \psi_1(x,y), \tag{28}$$

in which the terms $\varphi_1(x,y)$ and $\psi_1(x,y)$ can be determined by considering the closed-circuit case on the plate surfaces. By substituting Eqs. (5)-(7) into Eq. (2), the stress distributions are respectively

$$\begin{aligned}\sigma_x(x,y,z) = &-c_{11}A_{mn}zX_m''(x)Y_n(y) - c_{12}A_{mn}zX_m(x)Y_n''(y)\\ &-\left(e_{31}\frac{\Delta_1}{\Delta}+q_{31}\frac{\Delta_2}{\Delta}\right)A_{mn}z\left(X_m''(x)Y_n(y)+X_m(x)Y_n''(y)\right), \\ &+e_{31}\varphi_1(x,y)+q_{31}\psi_1(x,y)\end{aligned} \tag{29}$$

$$\begin{aligned}\sigma_y(x,y,z) = &-c_{12}A_{mn}zX_m''(x)Y_n(y) - c_{11}A_{mn}zX_m(x)Y_n''(y)\\ &-\left(e_{31}\frac{\Delta_1}{\Delta}+q_{31}\frac{\Delta_2}{\Delta}\right)A_{mn}z\left(X_m''(x)Y_n(y)+X_m(x)Y_n''(y)\right), \\ &+e_{31}\varphi_1(x,y)+q_{31}\psi_1(x,y)\end{aligned} \tag{30}$$

$$\tau_{xy} = -2c_{66}A_{mn}zX_m'(x)Y_n'(y). \tag{31}$$

The above equations provide the analytic solutions to the physical quantities of a magneto-electro-elastic thin plate subjected to surface applied load and can be decided according to the transverse deflection $w(x,y)$ and potential parameters $\varphi(x,y,z)$ and $\psi(x,y,z)$.

III. Numerical Demonstrations

In this section, some examples based on the proposed model for the thin magneto-electro-elastic rectangular plate subjected to external loads and closed-circuit electric restrictions are presented. For the first a few examples, the author demonstrates some special cases which have been verified in previous research works in order to validate the present study and tell the differences with other available literatures.

Mode shape validation. Since the mode shape corresponding to the free vibration of the MEE plate is of interest due to its importance on the nature and extent of the electro-magneto-mechanical coupling, we first check the validation of fundamental mode shapes for a piezoelectric square plate made of commonly used PZT4 material by utilizing the present model. In order to compare the results with those proposed by Heyliger & Saravanos [13], the dimensions of the plate are chosen to be $L_x/h=10$, $L_x=L_y$ and $h=0.01\,\mathrm{m}$, and the boundary conditions are assumed to be simply-supported around four edges with closed-circuit on the top and bottom surfaces, i.e. $\phi(x,y,-H/2)=\phi(x,y,-H/2)=0$. The thickness is normalized as $Z=z/H$, the displacements and electric potential are normalized with respects to their own largest values along thickness direction, i.e., $W=w/\max(w)$, $U=u/\max(u)$ and $\Phi=\phi/\max(u)$. The normalized distributions for both the transverse and in-plane mode shapes along with the electric potential for a PZT4 square thin plate are depicted in Fig. 1, as we can detect from this figure, it is almost identical to Fig. 2(a) in the paper conducted by Heyliger & Saravanos [13]. Therefore, good agreement has been reached.

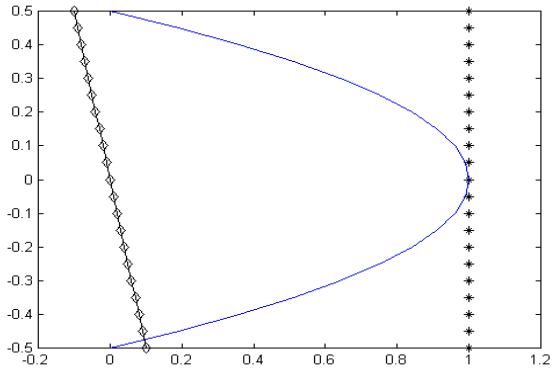

Fig 1. Thickness distributions for a PZT4 thin plate with dimension $L_x/h=10$, $L_x=L_y$ and $h=0.01\,\mathrm{m}$ subjected to simply-supported and closed-circuit boundary conditions.

Example 1. The second example is an electro-elastic single layer rectangular plate made of purely piezoelectric $BaTiO_3$. The length-to-thickness ratio and the width-to-thickness ratio are chosen to be $L_x/H = 10$ and $L_y/H = 5$ in order to match the dimension setting in the paper presented by Chen and Lee [6] although this doesn't assure the thin-plate requirement to be satisfied. All the surfaces of the plate are assumed to be traction free except the bottom surface, on which a sinusoidal loading $\Delta P=\sigma_0\sin(n\pi x/L_x)\sin(m\pi y/L_y)$ with amplitude $\sigma_0=1\,N/m^2$ and mode number $m=n=1$ is applied. In particular, the deformation responses of the plate are calculated at the fixed horizontal coordinates $(x_0,y_0)=(0.75L_x,0.25L_y)$. Fig. 2(a)-(f) indicates the variations along thickness direction of the elastic displacements w, u_x, u_y, electric potential $\phi(x,y,z)$, magnetic potential $\psi(x,y,z)$, electric displacement D_z and magnetic displacement B_z for such a plate caused by a sinusoidal loading on the top surface with all edges simply-supported. As we can recognize from these figures, the shear deformation is linearly dependent on the transverse deformation and the electric potential reveals quadratic variation along z coordinate. These two phenomena can be also found in both the papers studied by Pan [3] and Chen [6], see Fig. 1 and Fig. 2 in their studies respectively. It should be noted that the electric potential and magnetic potential in this case are identically zero due to the fact that $\frac{\partial D_z}{\partial z}=\frac{\partial B_z}{\partial z}=0$

and close-circuit electric restriction is adopted in this paper instead of open-circuit one.

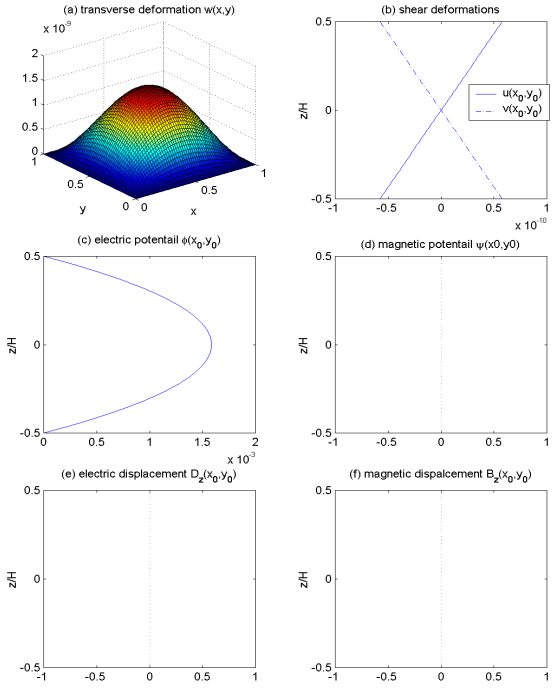

Fig. 2. Variations along thickness direction of the elastic displacements, electric potential, magnetic potential, electric displacement and magnetic displacement for a single layer BaTiO3 plate caused by sinusoidal loading on the top surface with all edges simply-supported.

Table 2. Material constants for both laminate and fibrous MEE multiphase composites, partially cited from Buchanan [12]

Material constants	PZT-4	$CoFe_2O_4$	Bi-layered $BaTiO_3$-$CoFe_2O_4$ laminate			$BaTiO_3$
v.f.	N.A.	0%	25%	50%	75%	100%
C_{11}	138.5	286	250	215	188	166
C_{12}	77.3	173	141	112	90	77
C_{13}	73.6	170	139	110	88	78
C_{33}	114.7	269.5	245	225	205	162
C_{44}	25.6	45.3	45	45	45	43
e_{31}	-5.2	0.0	0.0	0.0	0.0	-4.4
e_{33}	15.08	0.0	0.1	0.25	0.4	18.6
e_{15}	12.72	0.0	3.0	6.0	8.8	11.6
ε_{11}	1.306	0.08	3.4	6.3	8.8	11.2
ε_{33}	1.115	0.093	0.2	0.25	0.3	12.6
μ_{11}	5.0	-590	-4.45	-2.95	-1.55	5
μ_{33}	10	157	0.35	0.20	0.05	10
q_{31}	0	580.3	80	10	5	0.0
q_{33}	0.0	699.7	100	30	15	0.0
q_{15}	0.0	550	410	255	130	0.0
μ_{11}	0.0	0.0	-27500	-35500	-27000	0.0
μ_{33}	0.0	0.0	-24.5	-24.8	-23.5	0.0

(C_{ij} in 10^9N/m^2, e_{ij} in C/m^2, q_{ij} in N/Am^2, ε_{ij} in 10^{-9}C^2/Nm^2, and μ_{ij} in 10^{-6}Ns^2/C^2 and m_{ij} in 10^{-12}Ns/VC)

Example 2. In this example, a two-layered magneto-electro-elastic plate made of equally-placed $BaTiO_3$-$CoFe_2O_4$ laminate is then presented. The piezoelectric $BaTiO_3$ is placed on the bottom layer ($-H/2 < z < 0$) whereas the magnetostrictive $CoFe_2O_4$ is on the top layer ($0 < z < H/2$), the material constants for this kind of MEE plate can be found in Table 2 with the volume-fraction set to be 50% for the lamination case. The dimensions are $L_x = 1000$ m, $L_y = 20$ m, $h = 1$ m, $S \equiv L_y / h = 20$, $n = 1$ and the related physical quantities are normalized as follows with all of them still remain dimensional, u/S^3, v/S^3, $w \times 100/S^4$, σ_{xx}/S^2, σ_{yy}/S^2, σ_{xy}/S^2, ϕ/S^2, ψ/S^2, D_z/S, and B_z/S. The deformation variations of the magneto-electro-elastic plate due to external load, $\Delta P(x,y) = P_0 \sin \pi y / L_y$, applied on the top surface with magnitude $P_0 = 1\,\mathrm{N/m^2}$ are presented in Fig. 3 at the location $(x_0, y_0) = (L_x/2, S/4)$. Fig. 3(a)-(h) are the variations of the elastic displacements components $w(x,y)$ and $u_y(x_0, y_0, z)$, electric potential $\phi(x_0, y_0, z)$, magnetic potential $\psi(x_0, y_0, z)$, electric displacement D_z, magnetic displacement B_z, the normal stress components $\sigma_{11}(x_0, y_0, z)$ and $\sigma_{22}(x_0, y_0, z)$ along the thickness direction with boundary condition to be simply-supported around four edges. From these figures, we can obviously observe the interactive behavior between the piezoelectric, piezomagnetic and magnetoelectric effects for a magneto-electro-elastic (MEE) plate under mechanical applied load. If the MEE plate is assumed to be very thin, the deformation variations for both the electric and magnetic potentials reveal a quadratic dependence on the thickness variable, however, for the other related quantities such as shear deformations, electric and magnetic displacements as well as the stress distributions, linear dependence can be still detected.

From now on, the bi-layered $BaTiO_3$-$CoFe_2O_4$ laminate working as a magneto-electro-elastic plate will be discussed based on the Kirchoff hypothesis and the thin-plate theory. The simplified governing equation, Equation (1), will be examined subjected to various kinds of surface applied load, and the deformation behavior with different boundary conditions imposed on the plate will also be inspected. Due to the simplicity of the proposed model, the higher mode response can be easily performed; therefore, the deformation variation of the MEE plate with respect to different mode numbers will be carried out as a reference.

The dimensions of the MEE plate is set to be $L_x \times L_y \times H = 1\mathrm{m} * 1\mathrm{m} * 0.05\mathrm{m}$ unless otherwise mentioned, however, any kind of dimensions can be applied as long as the span-to-thickness ratio is satisfying the requirement for thin-plate theory, i.e., $L_x / H > 10$. The plate surfaces are assumed to be traction free except on the top or bottom surface, on which a z-direction surface load is applied. The external load can be of any type possibly occurs in the study of MEE plate, however, in order to observe the variation of the deformations, three commonly seen static forces are performed in this paper. They are

(1) uniform load, i.e., $P(x,y) = P_0$,

(2) distributed load, i.e., $P(x,y) = P_0 X_M(x) Y_N(y)$ and

(3) concentrated load, i.e., $P(x,y) = P_0 \delta(x - x_0, y - y_0)$.

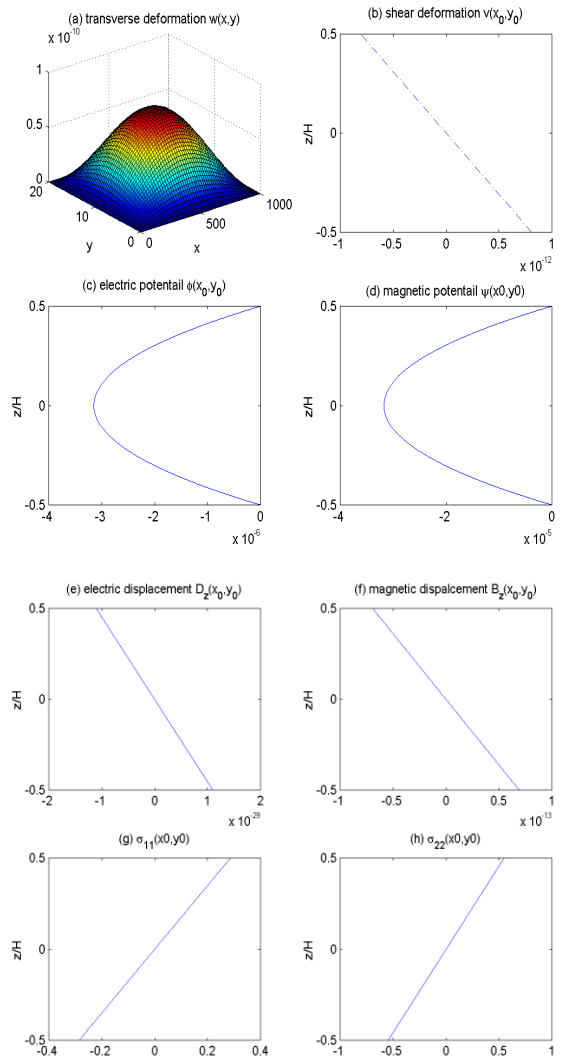

Fig. 3. Variations of the elastic displacements, electric potential, magnetic potential, electric displacement, magnetic displacement and normal stress components along the thickness direction for a two-layered magneto-electro-elastic BaTio3-CoFe2O4 plate caused by external loading on the top surface with all edges simply-supported.

The geometric boundary conditions imposed on the MEE plate can be any one of the combinations for free, clamped and simply-supported edges; however, in this study, only the boundary conditions of simply-supported around, clamped around and cantilever plates are conducted as numerical examples. It should be noted that the deformation responses for the MEE plate under static loads will be calculated at a fixed horizontal coordinate (x_0, y_0), however, due to the different plate characteristic with respect to different boundary conditions, the horizontal coordinates will be various according to the corresponding boundary conditions. That is, for SSSS plate location is chosen to be at $(x_0, y_0) = (0.5L_x, 0.5L_y)$, for CCCC plate at $(x_0, y_0) = (0.5L_x, 0.5L_y)$ and for CFFF plate at $(x_0, y_0) = (L_x, 0.5L_y)$.

Fig. 4 (a)-(d) are the deformation variation of electric potential, magnetic potential, electric displacement and magnetic displacement for the laminated $BaTiO_3$-$CoFe_2O_4$ MEE plate with simply-supported around edges and surface distributed load $\Delta P = \sin(\pi x / L_x)\sin(\pi y / L_y)$ with respect to various volume fraction of BaTiO3. As it can be observed, the concavity for the pure piezoelectric $BaTiO_3$ plate (v.f.=100%) is uniquely different from the other MEE laminates with a much higher magnitude. Although the dependence with respect to z variable remains quadratic, the electric potential for the MEE lamination with volume fraction other than 100% reveals a negative sign along the thickness direction instead of a positive one in the pure $BaTiO_3$ case. However, the magnitudes placed in order are 25%, 75% and 50%, 0% for the pure piezomagnetic CoFe2O4 case stands zero with no piezoelectric effect due to the applied load, which is quite reasonable. As for the magnetic potentials, quadratic relation can also be verified and the concavity for each case seems to be consistent. The maximum magnitude occurs in the 25% laminate followed by the 75%, 50% and 0% cases, 100% for pure piezoelectric $BaTiO_3$ case stays nil with piezomagnetic effect being vanished.

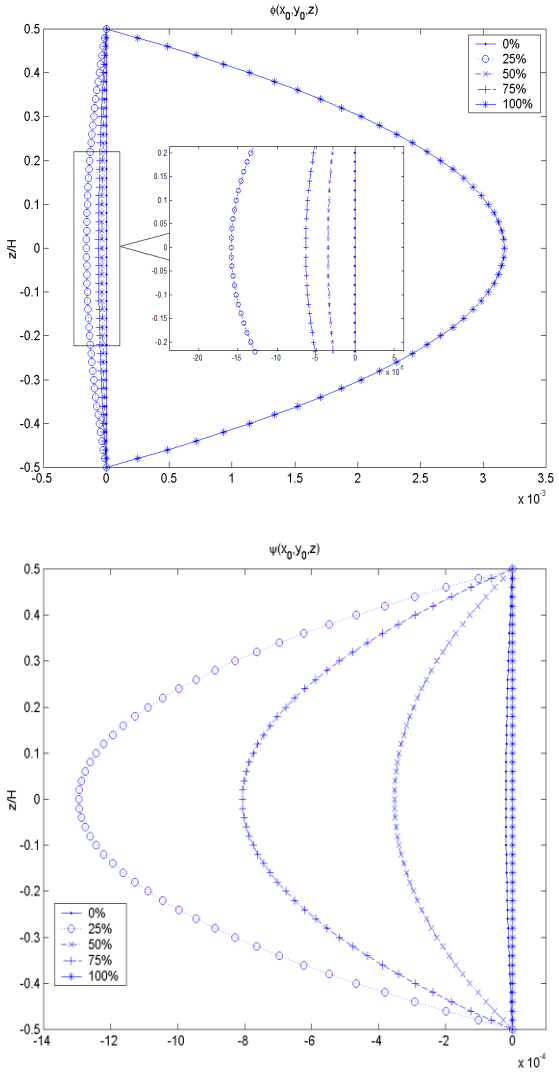

Fig. 4-1. Variation of (a) electric potential (b) magnetic potential for the lamination MEE plate with simply-supported BCs under surface distributed load.

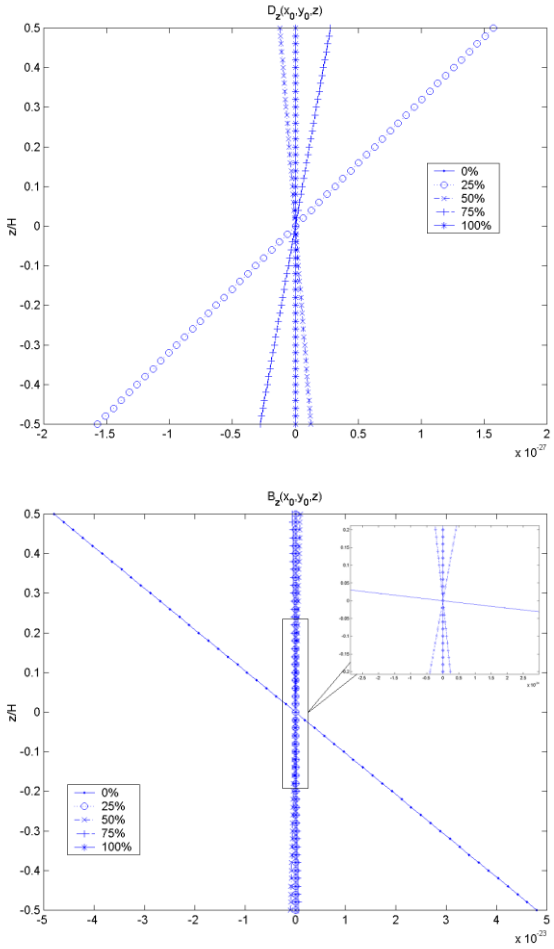

Fig. 4-2. Variation of (c) electric displacement (d) magnetic displacement for the lamination MEE plate with simply-supported BCs under surface distributed load.

For the MEE laminate presented in Fig. 4, the electric and magnetic displacements, also called fluxes, can be found to be linearly dependent on the z variable and the slope varies slightly with respect to the volume fraction of the MEE plate. However, if we near watch the magnitudes, we can find that all of them are pretty slim. This is due to the nature of the material parameter itself, also because of the close-circuit restriction we impose on the model. Nevertheless, if the electric and magnetic boundary conditions are chosen otherwise, the magnitudes for electric and magnetic displacements may be changed in a different way. Whatsoever, in the present study, only the close-circuit MEE thin plate is considered, therefore the author hereafter leave out all the presentations and discussions for the electric displacement and the magnetic displacement due to their insignificant effects.

Since the deformation variations for the laminate MEE plates with clamped-around edges and under uniform applied load $\Delta P = 1\ \mathrm{N/m^2}$ are quite similar to those behaviors presented in Fig. 4, the author therefore skip these two case and directly go to the cases for the cantilever laminate and fibrous MEE plate. Also the deformation variations for the electric and magnetic displacements are neglected due to their small magnitudes both approaching to zero.

Fig. 5 (a)-(b) are the deformation variation of electric potential, magnetic potential versus volume fraction for a cantilever laminated $BaTiO_3$-$CoFe_2O_4$ plate subjected to unit impulse force acting on the location (x_0, y_0) , i.e., $\Delta P = 1 \cdot \delta(x - x_0, y - y_0)$. The deformation behavior of a cantilever MEE plate is quite similar to the corresponding one of a simply-supported MEE plate except for the concavity. Owing to the different characteristics of MEE plate with different boundary conditions and subjected to different types of applied load, the sign change on the concavity is reasonable and expected.

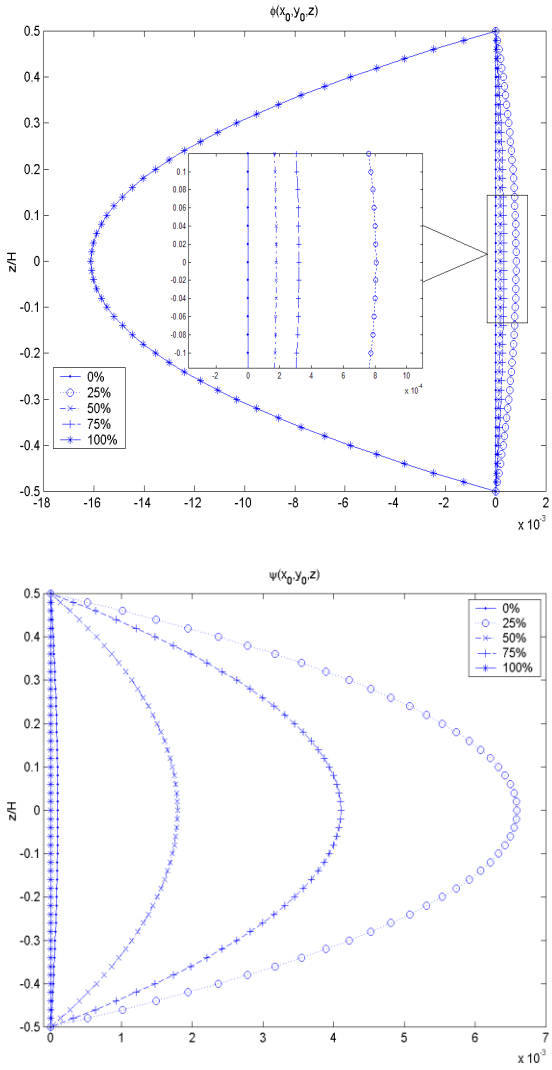

Fig. 5. (a)-(b) Deformation variation of electric potential and magnetic potential versus volume fraction for a cantilever laminated $BaTiO_3$-$CoFe_2O_4$ square plate subjected to unit impulse force acting on the location (x_0, y_0) , i.e., $\Delta P = 1 \cdot \delta(x - x_0, y - y_0)$.

The deformation variation of electric potential and magnetic potential for the 50% laminated $BaTiO_3$-$CoFe_2O_4$ MEE plates subjected to various loads with all edges simply-supported are demonstrated in Fig. 6 (a)-(b). And the corresponding deformation variations for the laminate MEE composites with all edges clamped are depicted in Fig. 7 (a)-(b). Followed by Fig. 8 (a)-(b), the same illustrations for the MEE cantilever plates are provided. As we can see from these figures, the concentrated applied load always stimulate much stronger deformation as we expected and followed by the distributed applied load, uniform applied load seems to be

less operative.

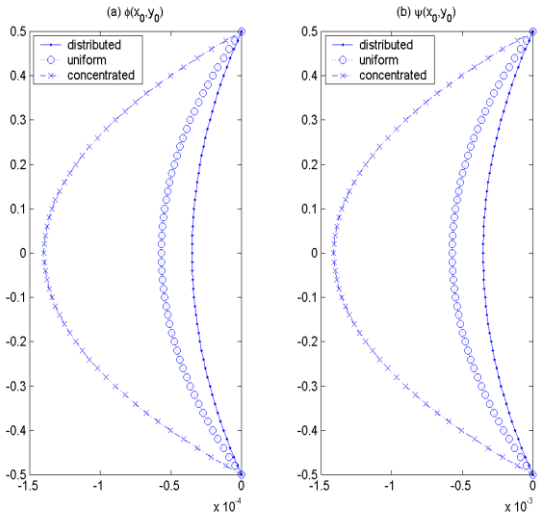

Fig. 6. (a)-(b) Deformation variation of electric potential and magnetic potential for the 50% laminated $BaTiO_3$-$CoFe_2O_4$ MEE plate subjected to various loads with all edges simply-supported.

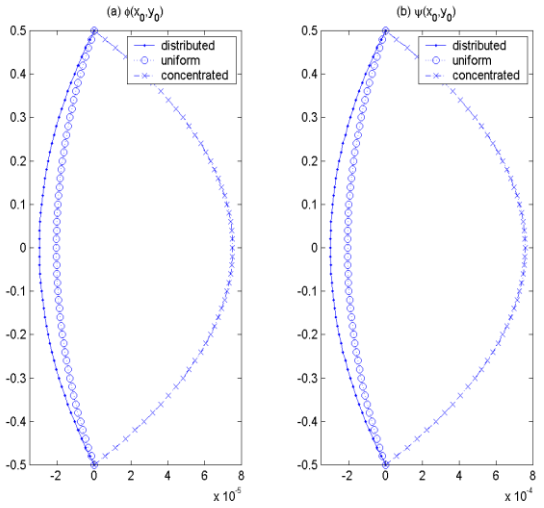

Fig. 7. (a)-(b) Deformation variation of electric potential and magnetic potential for the 50% laminated $BaTiO_3$-$CoFe_2O_4$ MEE plate subjected to various loads with all edges simply-supported.

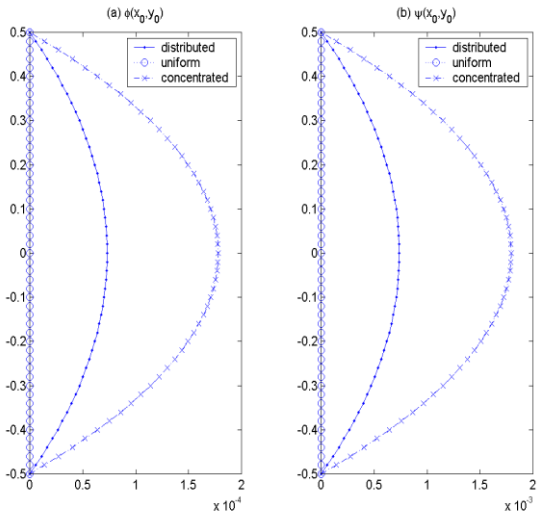

Fig. 8. (a)-(b) Deformation variation of electric potential and magnetic potential for the 50% laminated $BaTiO_3$-$CoFe_2O_4$ MEE cantilever plate subjected to various loads.

Finally, in order to see the influence of mode orders, the deformation variation of electric potential and magnetic potential versus mode number for the MEE laminate under certain applied load are given in Fig. 9 (a)-(b) with all edges simply-supported, in Fig. 10 (a)-(b) with all edges clamped, and in Fig. 11 (a)-(b) for the cantilever plate. It should be noted that some of the mode orders contributes nothing on the plate deformations because of maybe the symmetry of the mode shape or the location we calculate at.

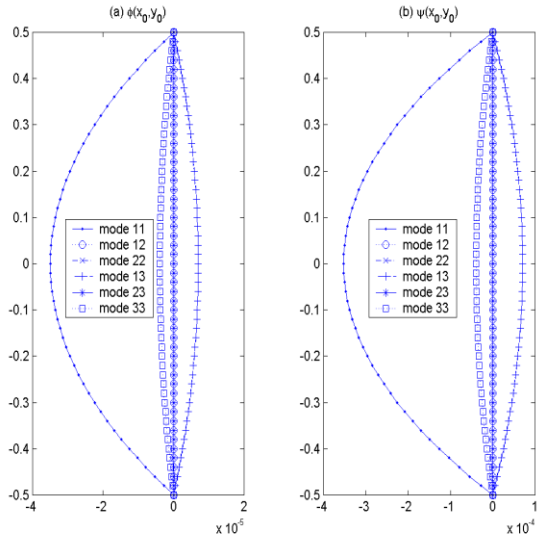

Fig. 9. (a)-(b) Deformation variation of electric potential and magnetic potential versus mode number for the 50% laminated $BaTiO_3$-$CoFe_2O_4$ MEE simply-supported plate subjected to sinusoidal loading.

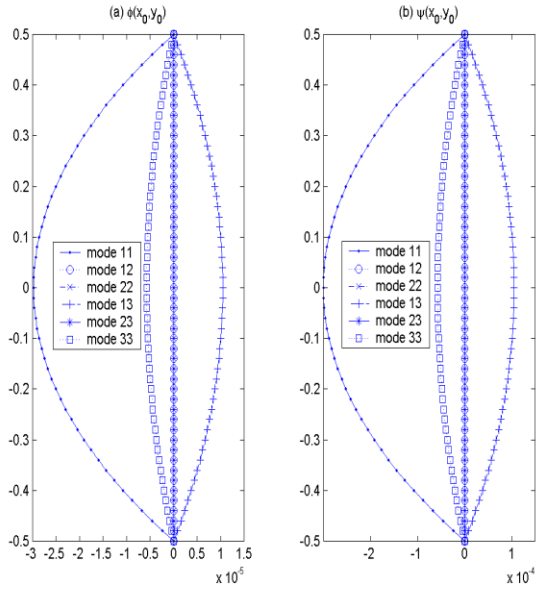

Fig. 10. (a)-(b) Deformation variation of electric potential and magnetic potential versus mode number for the 50% laminated $BaTiO_3$-$CoFe_2O_4$ MEE clamped plate subjected to sinusoidal loading.

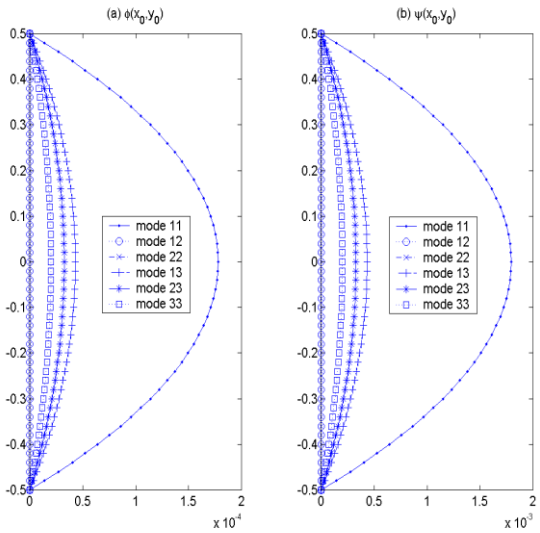

Fig. 11. (a)-(b) Deformation variation of electric potential and magnetic potential versus mode number for the 50% laminated $BaTiO_3$-$CoFe_2O_4$ MEE cantilever plate subjected to sinusoidal loading.

IV. Conclusion

The closed form solutions for the bending problem of a bi-layered $BaTiO_3$-$CoFe_2O_4$ composite are derived based on a new invented governing equation for magneto-electro-elastic (MEE) rectangular thin plate, in particular, the elastic displacements, electric potential and magnetic induction for a magneto-electro-elastic (MEE) laminate are implemented analytically.

It has been shown that the material coefficients for the MEE constituent vary a lot according to the volume-fraction of $BaTiO_3$ it contains. The deformation variations for the MEE thin plate with closed-circuit electric restriction are evaluated with respect to various boundary conditions, and the effects of the volume-fractions are investigated in detail. It can be found that the shear deformation is linearly dependent on the transverse deformation, whereas the electric and magnetic potential are both of quadratic variation along the thickness direction. In addition, the deformation behavior for a single phase material can be found to be quite different from the multiphase one in either the magnitude or the sign it is induced by.

The present study provides some commonly seen examples for the magneto-electro-elastic (MEE) rectangular thin plate under the action of 3 kinds applied loads, and offers the discrepancy on the deformation variation of electric potential and magnetic induction with respect to various typical boundary conditions. This work proposed a much easier and systematic way to seek for the analytic solutions for the deformation characteristics of a bi-layered MEE thin plate, and should be of interest to someone devoted on the practice of structure design with the fully coupled medium.

Acknowledgment

This work was partially supported by the National Science Council of the Republic of China under Grant NSC-95-2211-E327-046. The author is grateful for this support.

References

[1] Van Run AMJG, Terrel DR, Scholing JH. An in situ grown eutectic magnetoelectric composite material. Journal of Material Science 1974; 9(10):1710-1714.
[2] Li JY. Magnetoelectroelastic multi-inclusion and inhomogeneity and their applications in composite materials. International Journal of Engineering Science 2000; 38:1993-2011.
[3] Pan E. Exact solution for simply supported and multilayered magneto-electro-elastic plates. Transaction of the ASME Journal of Applied Mechanics 2001; 68:608-618.
[4] Chen ZR, Yu SW, Meng L, Lin Y. Effective properties of layered magneto-electro-elastic composites. Composite Structures 2002; 57:177-182.
[5] Wang X, Shen YP. The general solution of the three-dimensional problems in magnetoelectroelastic media. International Journal of Engineering Science 2002; 40:1069-1080.
[6] Chen WQ, Lee KY. Alternative state space formulations for magnetoelectric thermalelasticity with transverse isotropy and the application to bending analysis of non-homogeneous plates. International Journal of Solids and Structures 2003; 40:5689-5705.
[7] Wang JG, Chen LF, Fang SS. State vector approach to analysis of multilayered magneto-electro-elastic plates. International Journal of Solids and Structures 2003; 40:1669-1680.
[8] Ding HJ, Jiang AM. A boundary integral formulation and solution for 2D problems in magneto-electro-elastic media. Computers and Structures 2004; 82:1599-1607.
[9] Guan Q, He SR. Two-dimensional analysis of piezoelectric/piezomagntic and elastic media. Composite structures 2005; 69:229-237.
[10] Tzou HS. Piezoelectric Shells, Distributed Sensing and Control of Continua. Netherlands: Kluwer Academic Publishers, 1993.
[11] Liu MF, Chang TP. Closed form expression for the vibration problem of a transversely isotropic magneto-electro-elastic plate. Journal of Applied Mechanics-Transactions of The ASME 2010; 77: 024502-1-024502-8.
[12] Buchanan GR. Layered versus multiphase magneto-electro-elastic composites. Composites Part B 2004; 35:413-420.
[13] Heyliger P, Saravanos DA. Exact free-vibration analysis of laminated plates with embedded piezoelectric layers. The Journal of the Acoustical Society of America 1995; 98(3): 1547-1557.